CD Lab - Particulate Flow Modelling

Report
of the Liggghts-project

Implementation of a new rolling friction model

Author:

Andreas Aigner
andreas.aigner@jku.at

Supervisors:

DI Dr. Christoph Kloss

May 14, 2013

Contents

1 Introduction

In discrete element method (DEM) simulations the granular material is represented by perfectly shaped spheres. Since even the best and the stiffest real particles flatten slightly at the contact point to other particles or walls, they experience a torque counteracting the rotation. In the literature several rolling friction/rolling resistance models are presented that are capable to reproduce this effect. In the course of this study the model according to Ai et al. [1] is implemented, tested and compared to the current implementation in LIGGGHTS.

2 Rolling resistance models

This section provides a brief overview of the models [cf. 1]. Whereby both models use the *coefficient of rolling resistance* μ_r that is defined as a dimensionless parameter:

$$\mu_\mathrm{r} = \tan(\beta) \tag{1}$$

where β is the maximum angle of a slope on which the rolling resistance torque counterbalances the torque produced by gravity acting on the body.

2.1 Current implementation: Directional constant torque model

This model (also referred to as CDT-model) applies a torque against the relative rotation between the two contact entities. One has

$$M_\mathrm{r} = -\frac{\omega_\mathrm{rel}}{|\omega_\mathrm{rel}|}\mu_\mathrm{r} r_\mathrm{eff} F_\mathrm{n} \tag{2}$$

$$\omega_\mathrm{rel} = \omega_i - \omega_j \tag{3}$$

where ω_i and ω_j are the angular velocities of the particles i and j, respectively. Further ω_{rel} denotes the relative angular velocity, F_n is the normal force acting on the particle, and r_eff denotes the effective contact radius.

2.2 New implementation: Elastic-plastic spring-dashpot model

The model presented by Ai et al. [1] bases on the work of Jiang et al. [2] and is appropriate for both one way rolling and cyclic rolling cases. The total rolling resistance torque M_r consists of a spring torque M_r^k and a viscous damping torque M_r^d:

$$M_\mathrm{r} = M_\mathrm{r}^\mathrm{k} + M_\mathrm{r}^\mathrm{d} \tag{4}$$

At this point the governing equations are presented only. For more details the reader may be referred to Ai et al. [1].

$$\Delta M_\mathrm{r}^\mathrm{k} = -k_\mathrm{r}\Delta\theta_\mathrm{r} \tag{5}$$

$$M_{\mathrm{r,t}+\Delta\mathrm{t}}^\mathrm{k} = M_\mathrm{r,t}^\mathrm{k} + \Delta M_\mathrm{r}^\mathrm{k} \tag{6}$$

where the spring torque is limited by the torque at a full mobilisation rolling angle

$$|M_{\mathrm{r,t}+\Delta\mathrm{t}}^\mathrm{k}| \leq M_\mathrm{r}^\mathrm{m} \tag{7}$$

$$M_\mathrm{r}^\mathrm{m} = \mu_\mathrm{r} r_\mathrm{eff} F_\mathrm{n} \tag{8}$$

In this equations $\Delta\theta_\mathrm{r}$ denotes the incremental relative rotation between two particles and k_r stands for the rolling stiffness. The latter will be defined later.

The viscous damping torque M_r^d depends on the relative rolling angular velocity $\dot{\theta}_\mathrm{r}$ between the two contact partners and the damping constant C_r:

$$M_{\mathrm{r,t+\Delta t}}^\mathrm{d} = \begin{cases} -C_\mathrm{r}\dot{\theta}_\mathrm{r} & \text{if} |M_{\mathrm{r,t+\Delta t}}^\mathrm{k}| < M_\mathrm{r}^\mathrm{m} \\ -fC_\mathrm{r}\dot{\theta}_\mathrm{r} & \text{if} |M_{\mathrm{r,t+\Delta t}}^\mathrm{k}| = M_\mathrm{r}^\mathrm{m} \end{cases} \tag{9}$$

In course of this study the term f is set to 0. In practice it can be treated as a function of $\dot{\theta}_\mathrm{r}$ or $M_{\mathrm{r,t+\Delta t}}^\mathrm{d}$ in various different forms.

The rolling viscous damping coefficient C_r may be expressed as:

$$C_\mathrm{r} = \eta_\mathrm{r} C_\mathrm{r}^\mathrm{crit} \tag{10}$$

$$C_\mathrm{r}^\mathrm{crit} = 2\sqrt{I_\mathrm{r} k_\mathrm{r}} \tag{11}$$

$$I_\mathrm{r} = \left(\frac{1}{I_i + m_i r_i^2} + \frac{1}{I_j + m_j r_j^2} \right)^{-1} \tag{12}$$

where η_r is the rolling viscous damping ratio, I_i and I_j are the moment of inertia with respect to the centroid and m_i and m_j are the mass of the particles i and j, respectively.

2.2.1 The rolling stiffness k_r

In case of 2D simulations Ai et al. [1] suggest a rolling stiffness related to the normal contact stiffness k_n using

$$k_\mathrm{r} = 3k_\mathrm{n}\mu_\mathrm{r}^2 r_\mathrm{eff}^2 \tag{13}$$

They refer to the work of Jiang et al. [2], who defined the rolling stiffness as (rewritten in the notation used in this study)

$$k_\mathrm{r} = \frac{k_\mathrm{n}(2r_\mathrm{eff})^2}{12}\delta^2 = \frac{k_\mathrm{n} r_\mathrm{eff}^2}{3}\delta^2 \tag{14}$$

where 'the quantity δ is a dimensionless material and geometrical parameter which will generally be related to grain shape, and which we shall call the *shape parameter*.' [2]

Those two definitions leads to the never mentioned and elusive relation

$$\frac{\delta}{3} = \mu_\mathrm{r}. \tag{15}$$

Apart from that we may use instead of a straight line for 2D-particles (like in [2]) a plain circle with the diameter $d_\mathrm{c} = 2\delta \cdot r_\mathrm{eff}$ as contact area of two three-dimensional spheres. The spring torque is calculated by

$$M_\mathrm{r}^\mathrm{k} = \int_0^{\delta\, r_\mathrm{eff}} \int_0^{2\pi} k_\mathrm{n}^* \theta_\mathrm{r} x^3 \cos^2(\phi)\, \mathrm{d}\phi\, \mathrm{d}x \tag{16}$$

$$= \frac{\pi k_\mathrm{n}^* r_\mathrm{eff}^4}{4}\delta^4\theta_\mathrm{r} = \underbrace{\frac{k_n r_\mathrm{eff}^2}{4}\delta^2}_{k_\mathrm{r}}\,\theta_\mathrm{r} \tag{17}$$

with the normal stiffness per unit area k_n^* that is related to the normal stiffness used previously by $k_\mathrm{n} = k_\mathrm{n}^* \delta^2 r_\mathrm{eff}^2 \pi$.[1]

Finally, it follows from the equations (15) and (17) that the rolling stiffness of three-dimensional spheres can be calculated by

$$k_\mathrm{r} = \frac{9}{4} k_\mathrm{n} \mu_\mathrm{r}^2 r_\mathrm{eff}^2 \tag{18}$$

[1] In Jiang et al. [2] the contact width is defined as $B = \delta \cdot 2r_\mathrm{eff}$ and further on the normal stiffness is $k_\mathrm{n} = k_\mathrm{n}^* B$, since they investigated 2D problems only.

3 Implementation and usage

In this section the implementation of the model from section 2.2 is discussed in detail. In order to make the model available in most granular pair styles and granular wall styles, the model was mainly added to the functions *pair_gran_hooke_history* and *fix_wall_gran_hooke_history*. Additional coding was required only for the argument parsing in *fix_wall_gran_hertz_history*. In case of specialized pair styles like *pair_gran_hooke_history_hystereses* additional effort will be required, since those define their own compute_force and/or input argument parsing routines.

3.1 New input

The model 2.2 requires the rolling viscous damping ratio used in equation (10)) as one new *peratomtypepair* global parameter, which is defined by

```
fix     m7 all property/global coefficientRollingViscousDamping
    peratomtypepair 1 0.3
```

In order to use the EPSD-model an additional value *epsd* is available for the rolling_friction keyword, for instance

```
pair_style    gran/hertz/history rolling_friction epsd

fix    zwall all wall/gran/hertz/history primitive type 1 zplane 0.0
    rolling_friction epsd
```

3.2 Addition history values

The incremental increase of the spring torque in equation (6) involves to save either the total relative rotation θ_r of the two particles or the spring torque $M_{\mathrm{r,t}}^{\mathrm{k}}$ from the previous time step. Since for contact models with an time-dependent normal stiffness k_n, e. g. Hertz model, the rolling stiffness k_r and in further consequence the resulting torque are time-dependent too, saving the torque is the more general approach.

4 Test cases

Four different test cases are adopted in this study for model validation. All contacts are modelled by the Hertz contact model. Each uses the same material properties that are shown in table 1. The first one is part of the in-house material characterization procedure and is called 'inclined wall'. The other three test cases are recreated examples from the work of Ai et al. [1].

Parameter	Unit	Value
Particle radius (r)	(mm)	5
Young's modulus (Y)	(MPa)	40
Poisson's ratio (ν)		0.49
Density (ρ)	($\mathrm{kg/m^3}$)	1056
Friction coefficient (μ_s)		0.8
Rolling resistance coefficient (μ_r)		0.2
Viscous rolling damping ratio (η_r)		0.3
Time step (dt)	(s)	$1 \cdot 10^{-5}$

Table 1: Properties of the particles in test cases

Target angle (β)	$\mu_r = \tan(\beta)$	CDT model	EPSD model
4	0.06992	0.0688	0.0688
8	0.14054	0.14	0.13948
10	0.17632	0.17548	0.1752
15	0.26794	0.26704	0.26688
20	0.36397	0.36304	0.36288
25	0.46630	0.46547	0.46521
30	0.57735	0.576	0.576
35	0.70020	0.7	0.7

Table 2: Comparison of the results of test case 0

4.1 Test case 0: Inclined wall

This test case is designed to determine the coefficient of rolling friction for a given (measured) angle of an inclined wall, at which the particles start rolling. Since equation (1) links the same properties for the studied models, the result of our test case should agree the calculated coefficient of rolling friction of equation (1) for a given angle.

The simulation runs in a loop, while the coefficient of rolling friction decreases each run, until the particle starts to roll downwards. Deviating from the standard values from table 1 the viscous damping was disabled ($\eta_r = 0.0$) for the EPSD model in order to measure the point at which the rolling starts. A comparison of the predicted values of both models for several target angles is shown in table 2. Both models show a good agreement with the theoretical values.

REMARKS: With the chosen parameters both models fail to determine the rolling resistance coefficient for a target angle $\beta \geq 39°$. At this slope the particles start to slide down the wall. A higher friction coefficient would prevent this problem.

The CDT model predicts an oscillating torque why it is necessary that for the particle settling the threshold of the minimum kinetic energy is increased or the time step is decreased.

4.2 Test case 1: A single particle rolling on a flat surface

This case consists of one single particle rolling on a flat surface. The particle may settle under the influence of gravity on a rigid plate. After the particle has achieved equilibrium, an initial translational velocity $v_0 = 1.0\,\mathrm{m/s}$ and zero initial angular velocity is applied to it.

In figure 1 the rolling distance and the total torque acting on the particle are shown. The behaviour of the particle is very similar for both models, but the torque oscillates in case of the CDT model, when the particle reaches his final position (compare figure 1(a)).

4.3 Test case 2: A single particle rolling up a slope

The second test case simulates a single particle rolling up a rigid slope with an angle of 10° to the horizontal. This problem involves a continuous change of the potential energy. The set up is the same as in 4.2 but with the difference that the vector of gravitation is rotated about the 10° just before the initial velocity is applied to the particle.

Besides the oscillating torque the most remarkable difference between both models is that the CDT model can not prevent the particle from rolling down the slope at a very slow speed. The detailed view shown in figure 2 reveals the weak points of the CDT model. Furthermore, it can be seen that the EPSD model predicts the slightly back rolling of the particle before it becomes stationary.

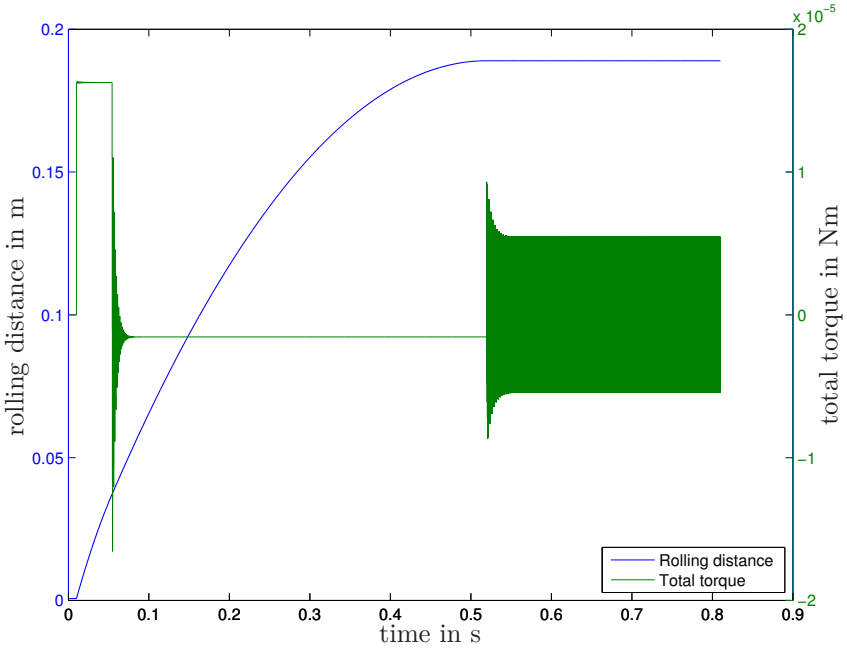

(a)

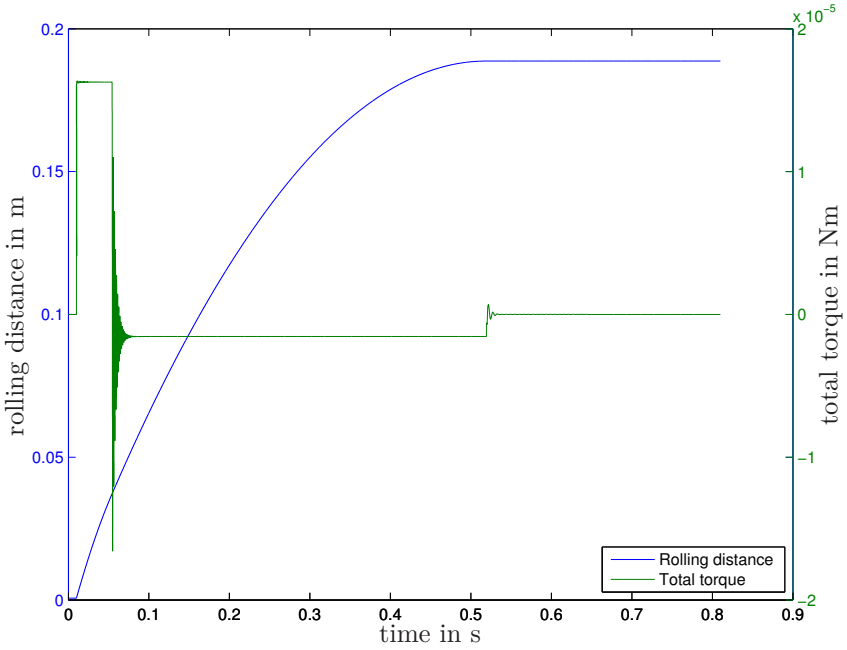

(b)

Figure 1: Rolling distance (x) and total torque (M_y) over time: (a) for the CDT model; (b) for the EPSD model.

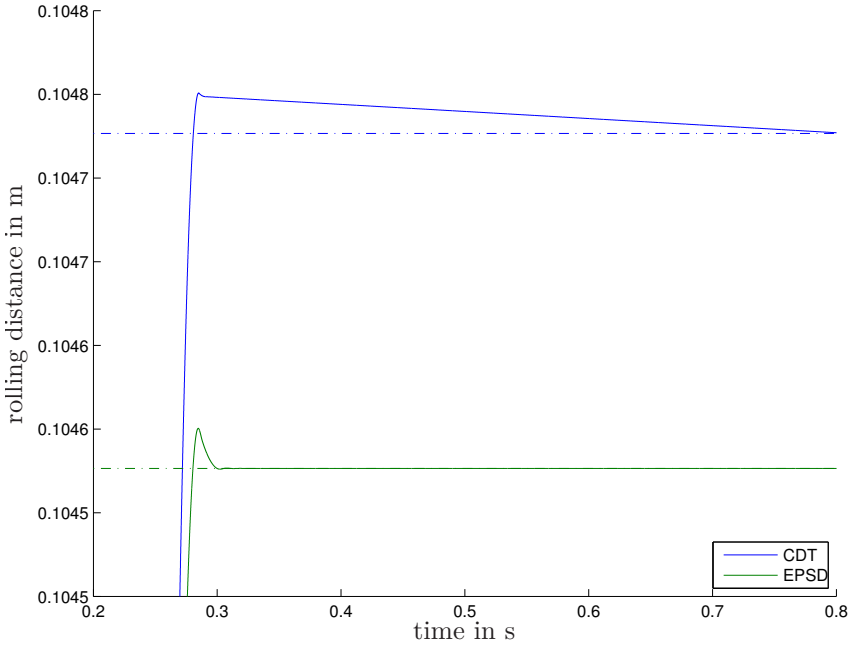

Figure 2: Rolling distance (x) over time. The particle simulated with the CDT model rolls down the slope at a very slow speed. The dash-dotted line indicates the horizontal.

4.4 Test case 3: Angle of repose

The last test case is a so called angle of repose experiment. Therefore, particles may settle inside a cylinder. After they have achieved equilibrium, the cylindrical wall is removed and the particle column collapses. Normally the angle of descent of the remaining, conical pile relative to the horizontal is measured for material characterization purposes. In course of this study the two models are compared with respect to their steady state behaviour. Therefore, we compare the total kinetic energy of all particles in the system after removing the sustaining wall. As shown in figure 3 the CDT model predicts a non-negligible kinetic energy also for the steady state situation due to the oscillating rolling torque. In contrary the finally achieved kinetic energy of the EPSD model is in the range of the numerical accuracy.

References

[1] Jun Ai, Jian-Fei Chen, J. Michael Rotter, and Jin Y. Ooi. Assessment of rolling resistance models in discrete element simulations. *Powder Technology*, 206(3):269–282, January 2011.

[2] M.J. Jiang, H.-S. Yu, and D. Harris. A novel discrete model for granular material incorporating rolling resistance. *Computers and Geotechnics*, 32(5):340–357, July 2005.

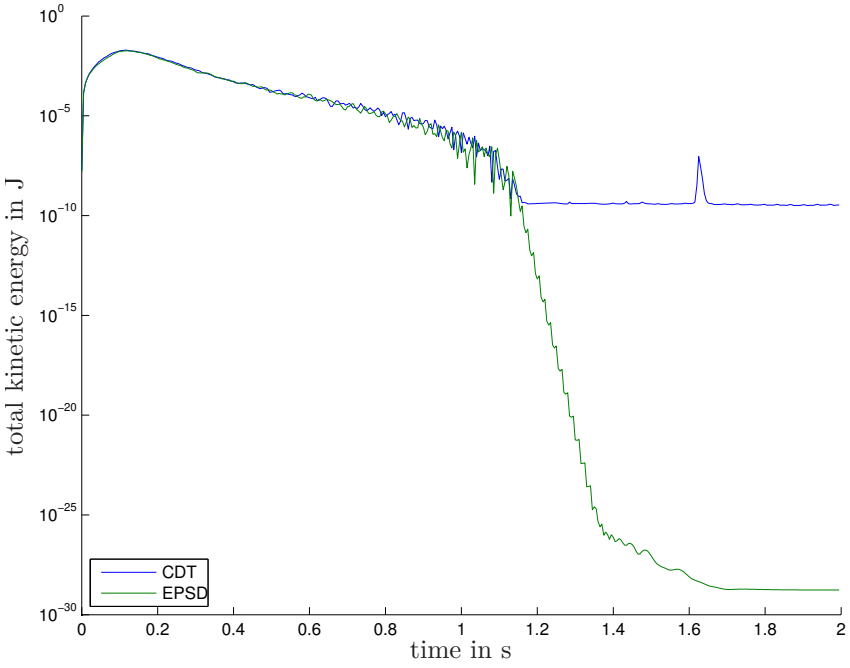

Figure 3: Total kinetic energy of all particles over time.